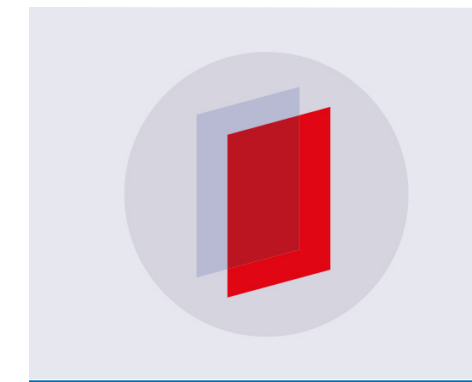
PAPER • OPEN ACCESS

The Evolution of Interplanetary Shocks Propagating into the Very Local Interstellar Medium

To cite this article: Parisa Mostafavi and Gary P. Zank 2018 J. Phys.: Conf. Ser. 1100 012018

View the article online for updates and enhancements.



IOP ebooks™

Bringing you innovative digital publishing with leading voices to create your essential collection of books in STEM research.

Start exploring the collection - download the first chapter of every title for free.

The Evolution of Interplanetary Shocks Propagating into the Very Local Interstellar Medium

Parisa Mostafavi^{1,2} and Gary P. Zank^{1,2}

[1] Department of Space Science, University of Alabama in Huntsville, Huntsville, AL 35899, USA

[2] Center for Space Plasma and Aeronomic Research (CSPAR), University of Alabama in Huntsville, Huntsville, AL 35899, USA

E-mail: psm0011@uah.edu

Abstract. Voyager 1 has made in situ measurements of the very local interstellar medium (VLISM) since August 2012 and its magnetometer and plasma wave instrument have detected several VLISM shock waves. Interplanetary shocks propagate through the supersonic solar wind and then through the inner heliosheath after colliding with the heliospheric termination shock (HTS). Interplanetary shock waves are transmitted partially across the heliopause (HP) into the VLISM and partially reflected back into the inner heliosheath. Previous studies showed that the in situ VLISM shocks observed by Voyager 1 were very weak and remarkably broad and had properties different than shocks inside the heliosphere [1, 2]. We model the first VLISM shock observed by Voyager 1 and compare with observations. We calculate the collisionality of the thermal particles and the dissipation terms such as heat conduction and viscosity that are associated with Coulomb collisions in the VLISM. The VLISM is collisional with respect to the thermal plasma and the VLISM shock structure is determined by thermal proton-proton collisions, which is the dominant thermal collisional term. The VLISM shock is controlled by particle collisions and not mediated by PUIs since they do not introduce significant dissipation through the shock transition. As a result, we find that the extremely broadness of the weak VLISM shock is due to the thermal collisionality.

Published under licence by IOP Publishing Ltd

Content from this work may be used under the terms of the Creative Commons Attribution 3.0 licence. Any further distribution of this work must maintain attribution to the author(s) and the title of the work, journal citation and DOI.

1. Introduction

The HP is a tangential discontinuity that separates plasma in the VLISM from solar wind plasma. Voyager 1 passed the HP and entered the VLISM at a distance of 121 AU on August 25, 2012, becoming the first human-made spacecraft to enter the VLISM and make in situ measurements. The Low Energy Charge Particle (LECP) instrument on Voyager 1 measures differential intensities of low energy particles over a range of energies. The LECP instrument showed an abrupt decrease in the number density of anomalous cosmic rays (ACRs) and termination shock particles (TSP), which are dominant in the inner heliosheath (IHS) [3]. The galactic cosmic ray intensity increases at the position of HP. These are the characteristics of the VLISM region [4–6]. We are unable to directly measure the plasma quantities of the VLISM since Voyager 1's plasma instrument stopped working after the Jovian encounter. However, the plasma wave instrument can be used to indirectly measure the electron number density from the frequency of electron plasma oscillations [3].

Gurnett et al. (2015) [2] found that abrupt changes in the magnetic field and electron density detected by Voyager 1 in the VLISM corresponded to shock waves. The observed frequency of shock waves in the VLISM is about one per year. The observed VLISM shocks are due to interplanetary shocks propagating outward from energetic solar events such as coronal mass ejections (CMEs). The CME-driven shocks propagate through the supersonic solar wind, collide with the HTS, causing it to move outward, and then propagate through the inner heliosheath, until the HP, where the shock is partially reflected to propagate back into heliosheath and partially transmitted into the VLISM [7–10]. Burlaga et al. (2013) [1] studied the first shock observed in the VLISM, finding that interstellar shocks possess properties quite different than heliospheric shocks. The VLISM shock was observed to have a weak jump in magnetic field, B, and appeared to correspond to a weak, low beta, and subcritical shock [11]. Using the coplanarity theorem Burlaga et al. (2013) [1] showed that the shock is quasi-perpendicular (the angle between shock normal and B is about 85°). Being highly perpendicular the very weak change in magnetic field across the shock corresponds to a compression ratio of about $B_2/B_1 \approx 1.4$ (here 2/1 refers to the downstream/upstream state of the shock). The shock wave is remarkable because of its smooth transition and very large width, being about 10^4 times broader than a shock with similar properties at 1 AU. The third shock observed in the VLISM in 2014 had similar properties as the first observed shock, being a weak, laminar, smooth, quasiperpendicular, and broad shock [2]. Thus far no theoretical explanation has been advanced to explain such a broad shock structure in the VLISM.

Collisional mean free paths in the heliosphere are very large. Collisionality can be neglected and therefore wave-particle interactions are important inside the heliosphere. Collisionless quasiperpendicular shocks dissipate energy over a length scale (i.e., ion inertial length scale) that is much less than the collisional length scale [12]. Collisionless shocks have been observed throughout the heliosphere. Here we show that the electron and proton collisional time scale in the VLISM is much smaller than the characteristic dynamical time scale in the VLISM and the corresponding collisional mean free paths are very small. Therefore, the VLISM is a collisional environment and shock waves propagating in it are collisional with respect to the thermal plasma. Thermal Coulomb collisions introduce dissipation terms such as heat conduction and viscosity into the system and these processes are responsible for determining the structure of VLISM shocks. Hot and fast neutral atoms created in the supersonic solar wind and IHS are deposited in the VLISM [13-15], and can experience secondary charge exchange with interstellar charged particles, which leads to the creation of suprathermal PUIs in the VLISM. The very small number density of VLISM PUIs compared to that of the thermal gas introduces a very small pressure in the VLISM. We show that the physical process determining the structure of a VLISM shock and the HTS is different. The HTS is mediated by PUIs and controlled by wave-particle interactions whereas VLISM shocks are controlled by particle collisions. In the following section, we derive the basic equations describing the VLISM environment and the structure of shock waves therein. We model the VLISM shock and compare with Voyager 1 observations in Section 3. Finally, we conclude and summarize our results.

2. The VLISM

The VLISM consists of interstellar neutral atoms, thermal electrons and protons, and suprathermal PUIs. The charge exchange mean free path of protons and hydrogen atom in the VLISM is significantly larger than the scales of interest and we can neglect their coupling. Zank et al. (2014) [14] calculated collisional time scales between PUIs that are created by secondary charge exchange and thermal VLISM electrons and protons in the VLISM and showed that PUIs are not equilibrated with background thermal electrons and protons on a scale less than 75 AU. PUIs should therefore be treated as a separate component in the system. PUIs scatter off

doi:10.1088/1742-6596/1100/1/012018

magnetic field fluctuations and drive streaming instabilities and experience pitch angle scattering that introduces a collisionless heat flux and a collisionless viscosity in the system. After using a collisionless Chapman-Enskog expansion, one can show the pressure tensor, P_I , and heat flux, q_I , terms assume the form,

$$\mathbf{P}_{\mathbf{I}} = P_{I}\mathbf{I} + \mathbf{\Pi}_{\mathbf{I}},\tag{1}$$

$$\Pi_{\mathbf{I}} = \begin{pmatrix}
1 & 0 & 0 \\
0 & 1 & 0 \\
0 & 0 & -2
\end{pmatrix} \frac{\eta_{k\ell}}{2} \left(\frac{\partial U_k}{\partial x_\ell} + \frac{\partial U_\ell}{\partial x_k} - \frac{2}{3} \delta_{k\ell} \frac{\partial U_m}{\partial x_m} \right), \tag{2}$$

$$q_I(x,t) = -\frac{1}{2} \mathbf{K}_I \cdot \nabla P_I, \qquad (3)$$

where $\Pi_{\rm I}$ is the stress tensor (i.e., collisionless viscosity) and $K_{\rm I}$ the diffusion coefficient (i.e., collisionless heat flux). The inclusion of $\Pi_{\rm I}$ and $K_{\rm I}$ is due to the nearly non-isotropic PUI distribution. Here, $P_{\rm I}$ is the PUI isotropic pressure, η is the PUI viscosity and U is the bulk flow velocity.

Thermal VLISM protons and electrons are assumed to have a nearly Maxwellian distribution function. The streaming collisional time scale of thermal charged particle "a" colliding with a stationary background population of thermal charged particles "b" can be calculated as

$$(\tau_s^{ab})^{-1} = \frac{n_b q_a^2 q_b^2 l n \Lambda}{2\pi \epsilon_0^2 m_a^2 V_{Ta}^3} \frac{m_b}{m_a} (1 + \frac{m_a}{m_b}) \frac{T_a}{T_b} \frac{G(x_b)}{x_a},\tag{4}$$

where G(x) is the Chandrasekhar function,

$$G(x) \equiv \frac{f(x) - xf'(x)}{2x^2}, \quad f(x) = \frac{2}{\sqrt{\pi}} \int_0^x e^{-z^2} dz = erf(x),$$
 (5)

f(x) is the error function and $x_{a/b} \equiv v/V_{Ta/b}$. $V_{Ta/b} = \sqrt{2K_BT_{a/b}m_{a/b}^{-1}}$ is the thermal speed, K_B is Boltzmann's constant, and $\ln \Lambda$ is the Coulomb logarithm. The n, q, m, and T for particles a and b denote number density, charge, mass, and temperature, respectively.

The VLISM thermal protons and electrons are collisionally equilibrated and have the same temperature of about 7500 K [16]. Therefore, the VLISM proton and electron thermal speeds are 11 $km\ s^{-1}$ and 477 $km\ s^{-1}$, respectively. The plasma wave instrument on Voyager 1

IOP Conf. Series: Journal of Physics: Conf. Series 1100 (2018) 012018 doi:10.1088/1742-6596/1100/1/012018

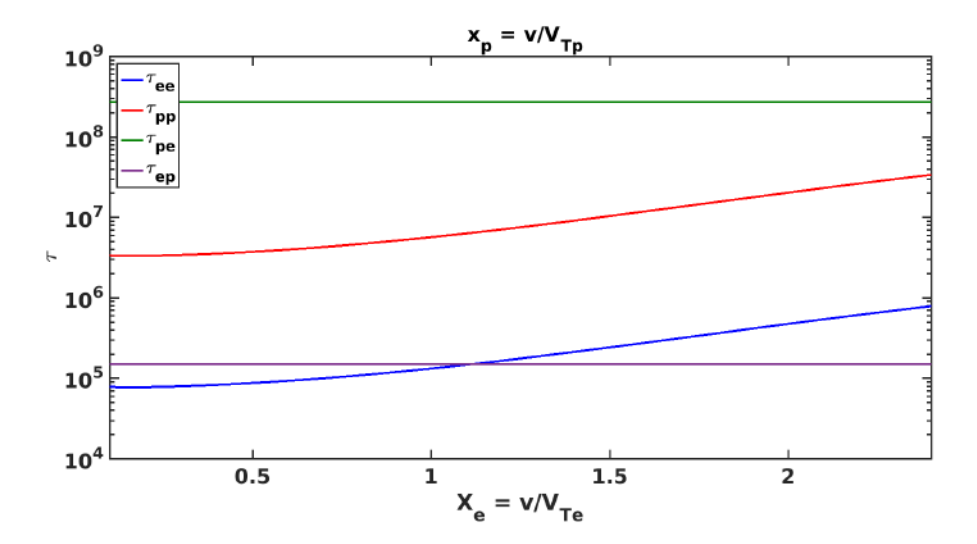


Figure 1: The pp, ee, ep, and pe collisional time-scales for the thermal VLISM plasma. Note that these collisional time scales do not apply to PUI collisional interactions with the thermal plasma.

measured the electron density upstream of the observed 2012 shock to be $0.06 \ cm^{-3}$ [2, 17, 18]. The magnetic field magnitude upstream of the VLISM shock measured by the magnetometer on Voyager 1 was about 0.38 nT [1]. We can evaluate the proton-proton (pp), electron-electron (ee), electron-proton (ep), and proton-electron (pe) collisional frictional time-scales and the mean free paths [10] for the region upstream of the observed VLISM shock using these parameters. Figure (1) shows the pp, ee, ep, and pe collisional time-scales for the thermal VLISM plasma as a function of velocity. Fig. (1) shows that the ep and pe collisional time-scales are independent of the velocity and constant,

$$\tau^{ep} = 1.5 \times 10^5 s$$
, $\lambda^{ep} = 0.47 AU$; $\tau^{pe} = 2.7 \times 10^8 s$, $\lambda^{pe} = 20.4 AU$, (6)

where τ is the collisional time-scale and λ is the mean free path. The time-scales for ee and pp collisions are not constant and depend on velocity. The collisional heat conduction and viscous coefficients depend on the collisional scattering time scales, τ_s , (see for example section §4.8 of [19]). We should estimate τ_s for pp and ee collisions and therefore we approximate an appropriate

doi:10.1088/1742-6596/1100/1/012018

collisional time, $\langle \tau_s \rangle$ as follows. The coefficient of viscosity, η , can be estimated as [14]

$$\eta \equiv \frac{4\pi}{3} \int c^2 \tau_s f_0 m c^2 dc, \tag{7}$$

where c = v - U is the random velocity. τ_s^{ee} and τ_s^{pp} can be approximated as 5^{th} degree polynomial curves from Fig. (1) and f_0 is a Maxwellian distribution. On integrating from 0 to $2.5V_T$, we obtain the viscosity coefficient, η , for ee and pp collisions. Using the pressure upstream of the VLISM shock and the relation $\eta \simeq P < \tau_s >$, we derive the most probable estimates

$$\tau^{pp} = 4.2 \times 10^6 s$$
, $\lambda^{pp} = 0.31 AU$; $\tau^{ee} = 7.5 \times 10^4 s$, $\lambda^{ee} = 0.24 AU$. (8)

Since the electron and proton collisional mean free paths are small compared to the almost featureless VLISM, we conclude that the VLISM is collisional with respect to the thermal plasma. The thermal gas Coulomb collisions introduce dissipation terms such as thermal heat conduction, K_g , and viscosity, η_g , (see [19] pages 159 – 161) in the VLISM region and therefore these collisional dissipation terms determine the structure of VLISM shocks.

Shock waves can be ideally modeled by considering a multi-fluid model for non-thermal PUIs, thermal protons, and thermal electrons. However, in most cases solving the multi-fluid model is very complicated and by making some assumptions it can be reduced to a single-fluid-like model (see [14, 15] for more details). The single-fluid-like system of equations comprises an equilibrated thermal plasma (electrons and protons) and a non-equilibrated PUI component. As was shown by Zank et al (2014) [14] PUIs should be treated as a separate pressure component, P_I , in the VLISM since they are not equilibrated with the background plasma. Taking into account that the bulk flow speed is dominated by protons and the electron mass is much smaller than the proton mass (details in [14, 15, 20, 21]), we can introduce the total density $\rho = m_e n_e + m_p n_p$, where the number density, n_p , includes both thermal protons and PUIs. The thermal gas pressure, P_g , contains both thermal proton and electron contributions, $P_g = P_e + P_p = n_e K_B T_e + n_p K_B T_p$. Here $n_{e/p}$, $P_{e/p}$, and $T_{e/p}$ are the thermal electron and proton number density, pressure, and temperature, respectively. The reduced single-fluid model comprises the continuity, momentum,

IOP Conf. Series: Journal of Physics: Conf. Series 1100 (2018) 012018 doi:10.

doi:10.1088/1742-6596/1100/1/012018

and energy equations, together with Maxwell's equations,

$$\frac{\partial \rho}{\partial t} + \nabla \cdot (\rho \mathbf{U}) = 0; \tag{9}$$

$$\rho(\frac{\partial \mathbf{U}}{\partial t} + \mathbf{U} \cdot \nabla \mathbf{U}) = -\nabla(P_g + P_I) - \nabla \cdot (\mathbf{\Pi}_I + \mathbf{\Pi}_g) + \mathbf{J} \times \mathbf{B}; \tag{10}$$

$$\frac{\partial P_g}{\partial t} + \mathbf{U} \cdot \nabla P_g + \gamma_g P_g \nabla \cdot \mathbf{U} = \frac{1}{3} \nabla \cdot (\mathbf{K_g} \cdot \nabla P_g) - (\gamma_g - 1) \mathbf{\Pi_g} : (\nabla \mathbf{U}); \tag{11}$$

$$\frac{\partial P_I}{\partial t} + \mathbf{U} \cdot \nabla P_I + \gamma_I P_I \nabla \cdot \mathbf{U} = \frac{1}{3} \nabla \cdot (\mathbf{K_I} \cdot \nabla P_I) - (\gamma_I - 1) \mathbf{\Pi_I} : (\nabla \mathbf{U}); \tag{12}$$

$$\frac{\partial}{\partial t} \left(\frac{1}{2} \rho \mathbf{U}^2 + \frac{P_I}{\gamma_I - 1} + \frac{P_g}{\gamma_g - 1} + \frac{1}{2\mu_0} B^2 \right) + \nabla \cdot \left(\frac{1}{2} \rho \mathbf{U} U^2 + \frac{\gamma_I}{\gamma_I - 1} P_I \mathbf{U} + \frac{\gamma_g}{\gamma_g - 1} P_g \mathbf{U} \right)
+ \frac{1}{\mu_0} B^2 \mathbf{U} - \frac{1}{\mu_0} \mathbf{U} \cdot \mathbf{B} \mathbf{B} + \mathbf{\Pi}_{\mathbf{I}} \cdot \mathbf{U} - \frac{1}{\gamma_I - 1} \frac{\mathbf{K}_{\mathbf{I}}}{3} \cdot \nabla P_I + \mathbf{\Pi}_{\mathbf{g}} \cdot \mathbf{U} - \frac{1}{\gamma_g - 1} \frac{\mathbf{K}_{\mathbf{g}}}{3} \cdot \nabla P_g) = 0;$$
(13)

$$\mathbf{E} = -\mathbf{U} \times \mathbf{B}; \ \frac{\partial \mathbf{B}}{\partial t} = -\nabla \times \mathbf{E}; \ \mu_0 \mathbf{J} = \nabla \times \mathbf{B}; \ \nabla \cdot \mathbf{B} = 0.$$
 (14)

B and E denote the magnetic and electric fields. $\gamma_{I/g}$ are the adiabatic indices of the PUIs/thermal gas. All quantities pertaining to PUIs and thermal gas are denoted with the subscripts I and g, respectively. The one-dimensional form of the collisional thermal plasma stress tensor and collisionless PUI stress tensor may be expressed as $\Pi_{g/I} = -\frac{1}{3}\eta_{g/I} \frac{dU_x}{dx}$, where η_g is the thermal collisional viscosity coefficient and η_I is the collisionless PUI viscosity coefficient associated with magnetic fluctuations [14, 22] and is typically assumed to be constant.

To establish that we need to consider the collisional viscosity in the system, we assume initially that the only dissipation term in the VLISM is the thermal heat flux and we neglect thermal viscosity. The PUIs are assumed to behave adiabatically. The 1-D form of the perpendicular shock (i.e., $\mathbf{U} = (U_x, 0, 0)$, $\mathbf{B} = (0, 0, B_z)$) structure equation is a first-order ordinary differential equation

$$\frac{dy}{dx} = (\gamma_g - 1) \frac{U_{x1}}{3K_g} (y - 1)(y - y_A) \frac{M(y)}{N(y)},\tag{15}$$

doi:10.1088/1742-6596/1100/1/012018

where

$$M(y) = \frac{1}{2} y_A y_B (1 - y) - \frac{1}{2} (y + 1)(y - y_A)^2 + \frac{1}{M_{II}^2 (\gamma_I - 1)} \frac{(y^{1 - \gamma_I} - 1)}{(1 - y)} (y - y_A)^2$$

$$- \frac{1}{\gamma_I M_{II}^2} \frac{\gamma_g}{\gamma_g - 1} y \frac{(y^{-\gamma_I} - 1)}{(1 - y)} (y - y_A)^2 - \frac{1}{(\gamma_g - 1) M_{s1}^2} (y - y_A)^2 + \frac{\gamma_g}{\gamma_g - 1} y (y - y_A)^2$$

$$+ y_B (y - y_A) - \frac{1}{2} \left(\frac{\gamma_g}{\gamma_g - 1} \right) y_B y (y + 1 - 2y_A);$$

$$N(y) = (y - y_A)^3 - y_B (1 - y_A)^2 - \frac{1}{M_{II}^2} (y - y_A)^3 y^{-\gamma_I - 1}.$$

$$(17)$$

Here y is the inverse compression ratio, y_A and y_B are the inverse Alfvénic Mach numbers squared along the x and z directions, respectively. Equation (15) has two solutions. The first solution yields smooth transitions from an upstream state to a downstream state. These solutions represent the class of smoothed shocks mediated completely by the thermal gas heat flux. The second set corresponds to double-valued solutions that are not physical, and a smooth transition from upstream to downstream is impossible. In this case, heat conduction associated with the thermal gas is not sufficient to smooth the shock structure, and an extra thermal gas dissipation term (thermal viscosity) must be added to affect the shock transition. Figure (2) shows a plot of M_{s1}^{-2} as a function of y_B for the case of quasi-perpendicular shocks ($y_A = B_x^2/(\rho_1 U_{x1}^2 \mu_0) \to 0$). The diagram identifies the two regimes i.e., smoothed and a regime that requires a sub-shock. The observed VLISM shock has the following parameters, $M_{s1}^2 = 0.06$, and $y_B = 0.3$, which shows that the VLISM shock is not in the smooth transition region. Therefore, thermal viscosity has to be added to ensure a smooth shock structure and hence transition (see also [20, 21]).

Here, a one-dimensional, steady-state model in which all physical quantities depend on the x Cartesian coordinate system is used. The 1-D background plasma velocity and magnetic field are $U = (U_x, 0, 0)$ and $B = (0, 0, B_z)$. The one dimensional form of equations (10)-(12) that includes both thermal gas viscosity and heat conduction in normalized form is

$$\gamma_g M_{s1}^2 \frac{\partial y}{\partial \bar{x}} = -\frac{\partial}{\partial \bar{x}} (P_g' + P_1 P_I') - y_B \gamma_g M_{s1}^2 B_z' \frac{\partial B_z'}{\partial \bar{x}} + \frac{1}{3} \gamma_g M_{s1}^2 (Sch_g + Sch_I \frac{K_I}{K_g} \frac{\rho_I}{\rho_g}) \frac{\partial^2 y}{\partial \bar{x}}; \quad (18)$$

$$yP_1\frac{\partial P_I'}{\partial \bar{x}} + \gamma_I P_I' P_1 \frac{\partial y}{\partial \bar{x}} = \frac{1}{3} P_1 \frac{K_I}{K_g} \frac{\partial^2 P_I'}{\partial \bar{x}^2} + \frac{1}{3} (\gamma_I - 1) \gamma_g M_{s1}^2 Sch_I \frac{K_I}{K_g} \frac{\rho_I}{\rho_g} (\frac{\partial y}{\partial \bar{x}})^2; \tag{19}$$

$$y\frac{\partial P_g'}{\partial \bar{x}} + \gamma_g P_g' \frac{\partial y}{\partial \bar{x}} = \frac{1}{3} \frac{\partial^2 P_g'}{\partial \bar{x}^2} + \frac{1}{3} (\gamma_g - 1) \gamma_g M_{s1}^2 Sch_g (\frac{\partial y}{\partial \bar{x}})^2, \tag{20}$$

doi:10.1088/1742-6596/1100/1/012018

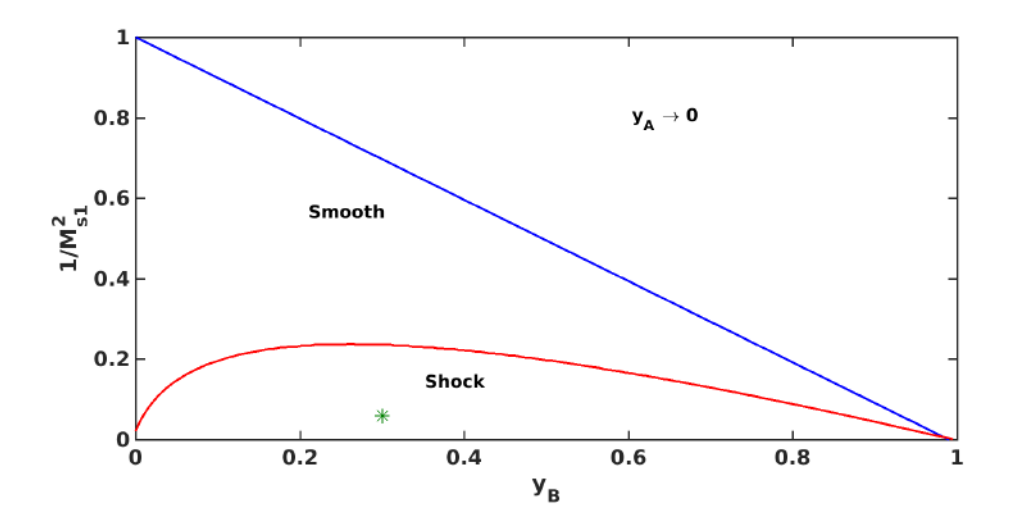


Figure 2: Initial upstream values M_{s1}^{-2} plotted as a function of y_B , for a quasi-perpendicular shock. The two regimes for which there is a smooth transition or a non-smooth (sub-shock) transition between the upstream and downstream states are identified. Here, $\gamma_I = \gamma_g = 5/3$ and $P_{I1}/P_{g1} = 0.05$. The green star corresponds to the parameters of the 2012 VLISM shock.

where $M_{s1}^2 = \rho_1 U_{x1}^2/\gamma_g P_{g1}$ is the thermal gas Mach number of the flow, $\bar{x} \equiv x/L$, $L \equiv K_g/U_1$, is distance normalized to the diffusion length scale, and $Sch_{g/I} \equiv \eta_{g/I}/(\rho_{1g/I}K_{g/I})$ is the Schmidt number of the thermal plasma/PUI. The inverse compression ratio is $y = U_x/U_{x1}$ and other normalized terms are defined as $P_g' = P_g/P_{g1}$, $P_I' = P_I/P_{I1}$, $B_z' = B_z/B_{z1}$, and $P_1 = P_{I1}/P_{g1}$. The inverse Alfvénic Mach number squared of the flow far upstream is expressed as $y_B = B_{z1}^2/(\rho_1 U_{x1}^2 \mu_0) = M_{Az0}^{-2}$.

The dominant collisional terms in a collisional magnetized plasma can be estimated by comparing the calculated thermal collisional mean free paths. We can neglect the electron-electron and electron-proton collisions. Since electrons have a very small mass compared to protons, they therefore do not contribute significantly to the dissipation process (i.e., thermal heat conduction or thermal viscosity) in the system. The large mean free path of proton-electron collisions compared to that of proton-proton collisions means that we can neglect proton-electron collisions. Thus the dominant collisional terms derive from proton-proton collisions and by using the expressions in Zank (2014) [19] (pages 159-161), the diffusion coefficient associated with

doi:10.1088/1742-6596/1100/1/012018

proton-proton collisions, K_{pp} , upstream of the observed VLISM shock can be calculated to be $10^{15} m^2 s^{-1}$, the thermal viscosity $2.5 \times 10^{-8} kgm^{-1} s^{-1}$, and the thermal Schmidt number is therefore about 0.25. The number density of PUIs inside the VLISM is very small [23] and they contribute a very small pressure compared to the thermal plasma $(P_{I1}/P_{g1} \approx 0.05)$. The pitch-angle scattering timescale in the VLISM is taken to be $3\times 2\pi\times \Omega_g^{-1}$, giving 5.17×10^2 s and the collisionless PUI heat conduction is calculated to be about $10^{14} m^2 s^{-1}$. The scattering time scale gives a value for the VLISM PUI viscosity, η_I , as $\sim 3.57 \times 10^{-13}~kg~m^{-1}s^{-1}$, making the PUI Schmidt number about 10^{-3} . The thermal gas Schmidt number is much greater than the PUI Schmidt number $(Sch_g >> Sch_I)$. Therefore as was shown by [20, 21], PUIs and the dissipation associated with them cannot mediate the VLISM shock and the PUI dissipation terms can be neglected compared to thermal gas dissipation terms. PUIs will therefore behave adiabatically and $P_I \rho^{-\gamma_I}$ is constant through a broad VLISM shock, and the thermal gas will be heated preferentially. However, this is completely different at the HTS. Zank et al. (1996) [13] predicted that the thermal gas remains relatively cold, with PUIs being heated through the HTS. The HTS observed by Voyager 2 confirmed this prediction and showed that the HTS is mediated by PUIs and reflected thermal protons do not provide a dissipation mechanism and are only heated adiabatically [24]. Thus the physical process determining the structure of the HTS and the VLISM shocks is very different.

The one-dimensional form of the model equations has been used to determine the structure of shocks in the VLISM, specifically the broad shock observed by Burlaga et al. (2013) [1]. One second-order ordinary differential equation in normalized form can be obtained from equations (18)-(20) for the structure of the VLISM shock,

$$\frac{d^2y}{d\overline{x}^2} + \frac{3}{Sch_g} \left[\left(\frac{\gamma_I}{\gamma_g} \frac{1}{M_{s1}^2} \left(\frac{1}{y} \right)^{\gamma_I + 1} - 1 \right) - Sch_g y + \frac{y_B}{y^3} \right] \frac{dy}{d\overline{x}} = \frac{9}{Sch_g} \frac{1}{M_{s1}^2} (1 - y) Z(y), \quad (21)$$

where

$$Z(y) \equiv M_{s1}^{2} \frac{\gamma_{g} + 1}{2} \left(y - \frac{\gamma_{g} - 1}{\gamma_{g} + 1} \right) - \left(1 + P_{1} - \frac{(\gamma_{I} - \gamma_{g})}{\gamma_{g}(\gamma_{I} - 1)} \frac{(1 - y^{1 - \gamma_{I}})}{(1 - y)} - \gamma_{g} M_{s1}^{2} \frac{y_{B}}{2y} \left(\frac{\gamma_{g} - 2}{\gamma_{g}} - y \right) \right). \tag{22}$$

Equation (21) is the shock structure equation in the presence of both thermal gas heat flux and viscosity. Further discussion related to the structure of VLISM shock waves was presented by

Mostafavi & Zank (2018) [25]. A related shock structure equation in the absence of the viscosity term was investigated by Webb (1983) [26].

3. Results

The angle between the shock normal and the magnetic field of the observed VLISM shock was 85 degrees which means the shock is highly perpendicular [1]. We assume the shock is perpendicular to model the VLISM shock. With the parameters observed upstream of the VLISM shock, the sound speed is $C_{s1} = 14 \text{ km s}^{-1}$ and the Alfvén speed is $V_{A1} = 34 \text{ km s}^{-1}$ ($C_s < V_A$). The magnetoacoustic speed of the ambient medium is 36.7 km s^{-1} which is consistent with the estimated magnetosonic speed given by [17], and yields a subcritical shock. The plasma beta upstream of the VLISM shock, which is the ratio between thermal gas pressure and magnetic field pressure, is about 0.2. Mellott (1985) showed that a low beta, low magnetosonic Mach number perpendicular shock is a laminar shock (see Fig. 1 of [27]). Burlaga et al. (2013) [1] found a weak jump of about 1.4 in the magnetic field intensity at the shock of late 2012 and showed that Voyager 1 (which is moving relative to the Sun at 17 km s^{-1}) moved past the broad VLISM shock in about 8.7 days. There are no observations of the VLISM shock propagation speed and therefore to simulate the VLISM shock we need to estimate a shock propagation speed. Since a subcritical shock has a magnetosonic Mach number less than about two, the upstream flow speed in the shock frame should be considered as less than 72 km s^{-1} and therefore, the shock speed in the stationary Sun frame should be less than 52 $km s^{-1}$ (assuming the VLISM flows toward the Sun with a speed of 20 km s^{-1}). Kim et al. (2017) [28] used near-Earth solar wind data to model interplanetary shock propagation beyond the HP with the Multi-Scale Fluid-Kinetic Simulation Suite (MS-FLUKSS) code. Their simulation shows that the shock observed at the end of 2012 had a compression ratio of about 1.65 and a shock speed of about 50 $km s^{-1}$ in a frame in which the Sun is stationary (private communication with Dr. Tae Kim). For our model, we adopt a shock speed of 40 $km s^{-1}$ with respect to the stationary Sun. The thickness of the VLISM shock is about 0.12 AU which corresponds to Voyager 1's traversal of the shock in 8.7 days. As noted by Burlaga et al (2013) [1] the thickness of the VLISM shock is much greater than that expected for a shock with similar properties in the solar wind at 1 AU. The VLISM proton-proton collisions upstream of the observed shock give values of the thermal heat conduction length scale, K/U_1 , and the viscous length scale, η/ρ_1U_1 , of about 0.115 AU and IOP Conf. Series: Journal of Physics: Conf. Series 1100 (2018) 012018 doi:10.1088/1742-6596/1100/1/012018

0.03 AU, respectively.

We solve equation (21) in the stationary frame of the shock to model the VLISM shock. Figure 3 shows a smooth transition connecting the upstream to the downstream state. Here the VLISM shock compression ratio is about 1.67, indicating a weak shock transition. The shock thickness is determined by proton-proton collisions and is about 0.12 AU. The change in magnetic field through the VLISM shock is shown in Fig. 4. Figure 5 shows the normalized pressure as a function of unnormalized distance (AU). The dominant components downstream of the VLISM shock are thermal gas and magnetic field pressure. The shock is not mediated by PUIs since they do not contribute a large pressure through the shock. The fast magnetosonic Mach number shows that the flow changes from supersonic to subsonic (Fig. 6). Here one can see, because PUIs do not contribute a large pressure through the shock, that the inclusion of PUIs in the sound speed does not change the magnetosonic Mach number much and they are are essentially the same. The last figure (Fig. 7) shows the change of thermal gas entropy and PUI entropy through the VLISM shock. Since PUIs are effectively heated adiabatically, the entropy is constant through the shock layer. However, the thermal gas is collisionally dissipated and its associated entropy increases at the shock position.

4. Conclusions

Since the thermal proton and electron collisional mean free paths in the VLISM are very small compared to the almost featureless VLISM, we conclude the VLISM is a collisional environment with respect to the thermal plasma. The thermal collisions, which are dominated by protonproton collisions, yield thermal collisional dissipation terms (heat flux and viscosity). PUIs outside the heliosphere are generated by secondary charge exchange and experience pitch angle scattering by magnetic fluctuations. They contribute a collisionless heat flux and collisionless viscosity (i.e., introduced by wave-particle interactions). However, we can neglect the PUI dissipation terms because the PUI Schmidt number is small compared to the thermal gas Schmidt number. We have shown that the dominant collisional term in the VLISM is protonproton collisions and thus the structure of the broad interstellar shocks observed by Voyager 1 is determined by interstellar proton-proton collisions. The VLISM shock is therefore the first in situ observed example of a classical collisional subcritical shock, which means the shock structure is not controlled by wave-particle interactions but by particle collisions. The weak shock is

doi:10.1088/1742-6596/1100/1/012018

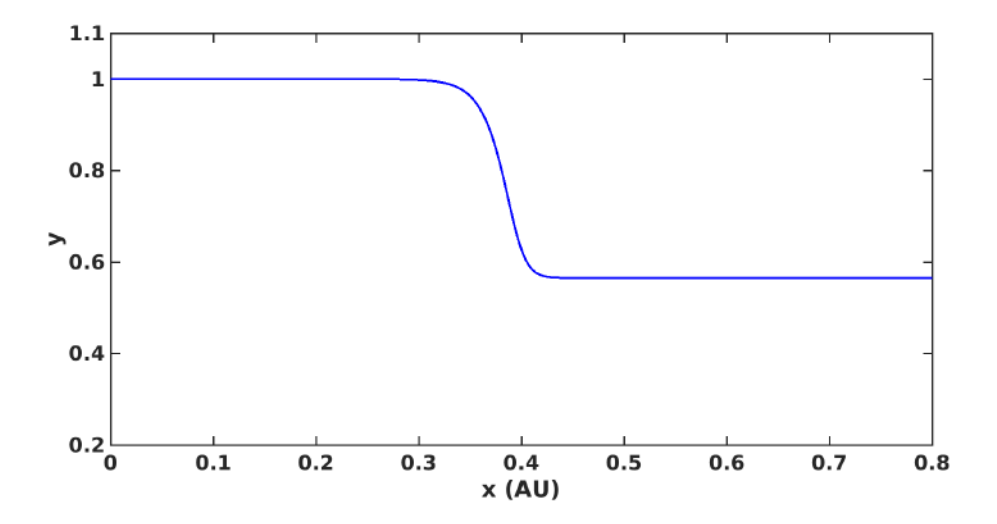


Figure 3: Inverse compression ratio as a function of unnormalized distance (AU) showing that the shock is smoothed. Here $\gamma_g = \gamma_I = 5/3$, $P_{I1}/P_{g1} = 0.05$, $y_B = 0.31$, and $M_{s1} = 4.17$.

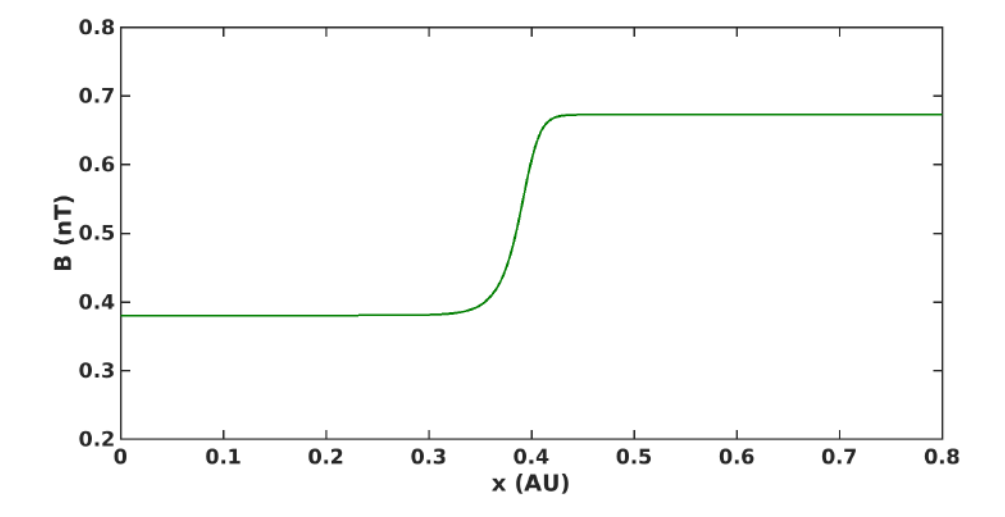


Figure 4: The unnormalized magnetic field (nT) through the shock as a function of unnormalized distance (AU) showing a weak compression in the magnetic field. Here $\gamma_g = \gamma_I = 5/3$, $P_{I1}/P_{g1} = 0.05$, $y_B = 0.31$, and $M_{s1} = 4.17$.

doi:10.1088/1742-6596/1100/1/012018

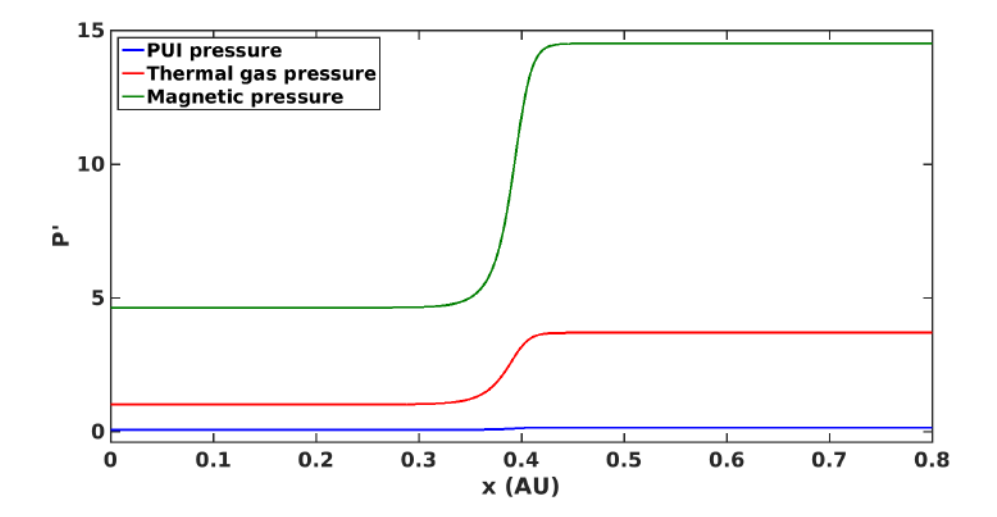


Figure 5: PUI, thermal gas, and magnetic pressure normalized to the thermal gas pressure far upstream as a function of unnormalized distance (AU).

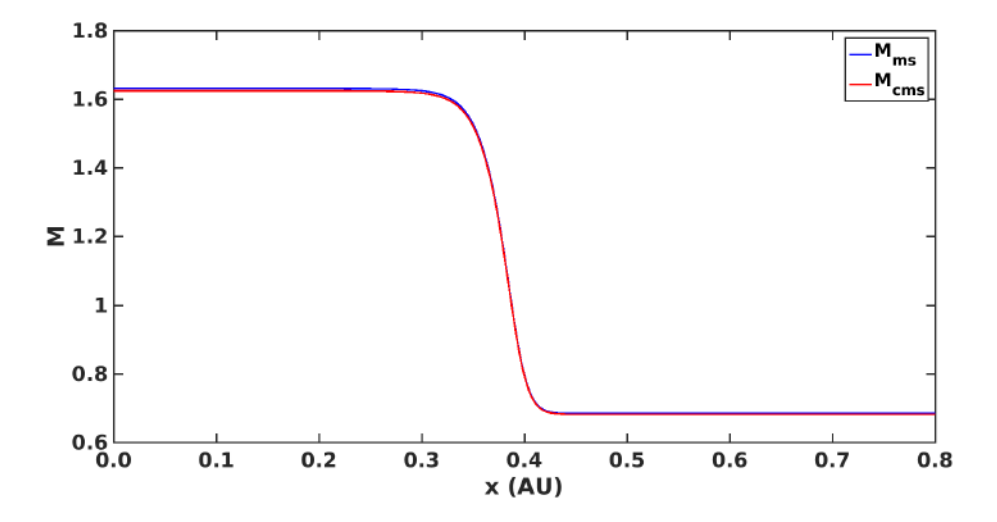


Figure 6: The magnetosonic Mach number as a function of unnormalized distance (AU). The thermal gas magnetosonic Mach number (blue line) and the combined effective thermal gas and PUI magnetosonic Mach number (red line) show that the flow changes from supersonic to subsonic.

doi:10.1088/1742-6596/1100/1/012018

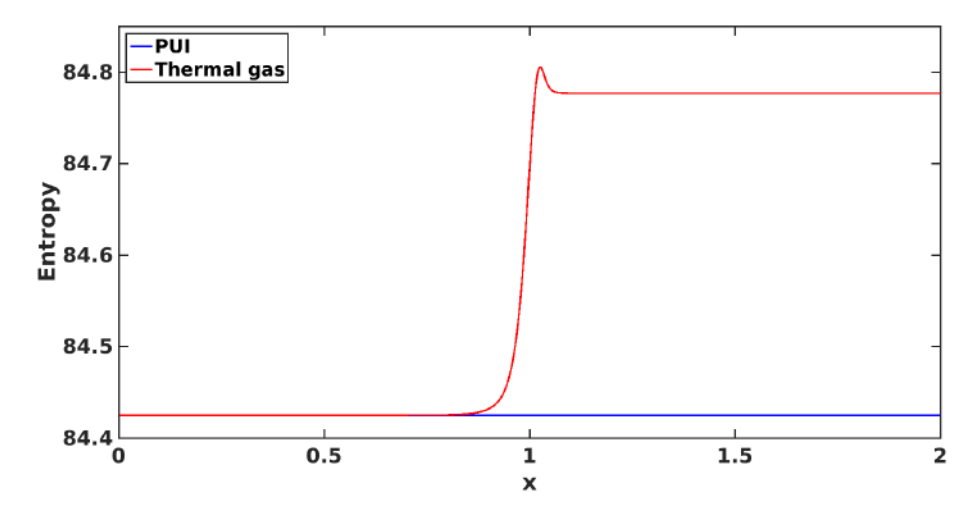


Figure 7: Entropy of thermal gas and PUIs through the VLISM shock as a function of normalized distance.

dominated by the magnetic field and thermal gas pressure whereas PUIs do not contribute a large pressure through the shock transition. Both the thermal and the combined thermal-PUI fast magnetosonic Mach number through the VLISM shock show that the flow changes from supersonic to subsonic. The overall thickness of the shock transition is about 0.12AU, which corresponds to the VLISM heat conduction length scale. Entropy associated with the thermal gas is not constant and increases at the position of a VLISM shock wave.

Acknowledgments

P.M. acknowledges the support of a NASA Earth and Space Science Fellowship Program-Grant 16-HELIO16F-0022. G.P.Z. acknowledges the support of NASA grants NNX14AC08G, NNX15AI65G, NNX17AB04G, NNX14AJ53G, and the NSF EPSCoR RII-Track-1 Cooperative Agreement OIA-1655280.

References

- Burlaga L F, Ness N F, Gurnett D A and Kurth W S 2013 The Astrophysical Journal Letters 778 L3
- [2] Gurnett D A, Kurth W S, Stone E C, Cummings A C, Krimigis S M, Decker R B, Ness N F and Burlaga L F 2015 The Astrophysical Journal 809 121
- [3] Gurnett D A, Kurth W S, Burlaga L F and Ness N F 2013 Science 341 1489–1492

- [4] Stone E C, Cummings A C, McDonald F B, Heikkila B C, Lal N and Webber W R 2013 Science 341 150–153
- [5] Krimigis S M, Decker R B, Roelof E C, Hill M E, Armstrong T P, Gloeckler G, Hamilton D C and Lanzerotti L J 2013 Science 341 144–147
- [6] Webber W R and McDonald F B 2013 Geophysical Research Letters 40 1665–1668
- [7] Whang Y C and Burlaga L F 1994 JGR 99 21
- [8] Zank G P and Müller H 2003 JGR 108 1240–+
- [9] Washimi H, Zank G P, Hu Q, Tanaka T, Munakata K and Shinagawa H 2011 MNRAS 416 1475–1485
- [10] Zank G P 2015 53 449–500
- [11] Mellott M M and Greenstadt E W 1984 JGR 89 2151–2161
- [12] De Hoffmann F and Teller E 1950 Phys. Rev. 80(4) 692-703 URL https://link.aps.org/doi/10.1103/PhysRev.80.692
- [13] Zank G P, Pauls H L, Cairns I H and Webb G M 1996 JGR 101 457–478
- [14] Zank G P, Hunana P, Mostafavi P and Goldstein M L 2014 The Astrophysical Journal 797 87
- [15] Zank G P, Mostafavi P and Hunana P 2016 Journal of Physics Conference Series 719 012014
- [16] McComas D J, Bzowski M, Frisch P, Fuselier S A, Kubiak M A, Kucharek H, Leonard T, Mbius E, Schwadron N A, Sok J M, Swaczyna P and Witte M 2015 The Astrophysical Journal 801 28 URL http://stacks.iop.org/0004-637X/801/i=1/a=28
- [17] Gurnett D A, Kurth W S, Burlaga L F and Ness N F 2013 Science 341 150-153
- [18] Gurnett D A, Kurth W S, Stone E C, Cummings A C, Krimigis S M, Decker R B, Ness N F and Burlaga L F 2014 AGU Fall Meeting Abstracts
- [19] Zank G P 2014 Transport Processes in Space Physics and Astrophysics (Lecture Notes in Physics, Berlin Springer Verlag vol 877)
- [20] Mostafavi P, Zank G P and Webb G M 2017 The Astrophysical Journal 841 4
- [21] Mostafavi P, Zank G P and Webb G M 2017 Journal of Physics: Conference Series 900 012016 URL http://stacks.iop.org/1742-6596/900/i=1/a=012016

- [22] Jokipii J R and Williams L L 1992 The Astrophysical Journal 394 184–187
- [23] Zirnstein E J, Heerikhuisen J, Zank G P, Pogorelov N V, McComas D J and Desai M I 2014 The Astrophysical Journal 783 129
- [24] Richardson J D, Kasper J C, Wang C, Belcher J W and Lazarus A J 2008 Nature 454 63 - 66
- [25] Mostafavi P and Zank G P 2018 The Astrophysical Journal Letters 854 L15 URL http://stacks.iop.org/2041-8205/854/i=1/a=L15
- [26] Webb G M 1983 American Astronomical Society 127 97–112
- [27] Mellott M M 1985 Washington DC American Geophysical Union Geophysical Monograph Series 35 131-140
- [28] Kim T K, Pogorelov N V and Burlaga L F 2017 The Astrophysical Journal Letters 843 L32 URL http://stacks.iop.org/2041-8205/843/i=2/a=L32